Hydrodynamic pressure and its effects on embedded tube tunnel in high permeable stratum

XiangHong CHEN, JianJun ZANG

China coal construction group co., LTD., Beijing, 100161 China

Email: 06115214@bjtu.edu.cn

Abstract. When dynamic loadings act on the embedded structure, vibration will be generated and transmitted to the surrounding ground causing dynamic deformation and stress of structure. A semi-analytical solution for hydrodynamic pressure of circular cavity in high permeable stratum using the conformal transformation method is proposed and the amplitude of hydrodynamic water pressure about the frequency is investigated under the harmonic vibration loadings. Furthermore, based on Kirchhoff - love assumption, considering the dynamic interaction of soil and tunnel structure, by means of numerical examples, the dynamic characteristics of a single embedded tunnel was analysed due to the hydrodynamic pressure, the calculation results show that, the vibration response of the tunnel structure is under the similar tendency for different water depth, but affected variously; the impedances of soil can significantly reduce the deformation and internal force of tunnel to a certain extent.

1. Introduction

In recent years, the construction of underground tunnel designed in complicated geological conditions will be faced by constructers and designers, so the stability of tunnel structure induced by stochastic vibration loadings of explosion, collision, oscillation became more serious, especially for the incidence of groundwater action in high permeable soil deposits, and the issue of hydrodynamic pressure and its effects on the tunnel lining need to be investigated.

Underground tunnel structure in high permeability medium will is designed to withstand the water pressures and earth pressures generated by vibration loadings. According to the water motion methodology, the simple closed-form analytical solutions of seepage force along the circular cavity circumference in the steady-state water flow conditions are derived (Park et al. [1,2]; Kolymbas et al. [3]; Huang Fu-ming [4]) by using the complex variable technique, the image well method (Harr [5]; Fernandez et al. [6]), the Mobius transformation and Fourier series by El Tani [7]. The effectiveness of seepage force on the stress and deformation of supporting structure are investigated mainly by numerical method (In-Mo Lee et al. [8,9]; Seok-Woo Nam et al. [10,11]; Carranza Torres et al. [12]; Zhang Zhi-qiang et al. [13]; Gao Xin-qiang et al. [14]). While, all the above analysis are only confined to the steady-state ground-water flow condition, as to the vibration-induced hydrodynamic pressure, the most common analytical tool is the decoupling method considering the soil-water interaction based on biot's theory (A Bobet [15,16]; Kang-he Xie et al. [17]; Gatmiri et al. [18]; Seyyed et al. [19]; Yi-Qun Tang et al. [20]), and the numerical method is often used to solve the whole system of soil-water and structure (Hashash et al. [21]; Taylor et al. [22]; Anastasopoulos et al. [23]; Amorosi et al. [24]).

When ignoring the soil and water interaction, the hydrodynamic pressure meeting with the Laplace wave equation can be deduced through the method of separation of variables. Westergaard firstly

investigated the earthquake-induced hydrodynamic pressure on an upright rigid dam. Furthermore this method was applied extendedly to the vertical plates and storage tanks (Kwak et al. [25,26]; J.Z Zhou et al. [27]) with vertical side wall.

According to the hydrodynamic pressure on curved side wall and its effects on structure, the focus is placed mainly at arch dam, immersed tunnel and submerged floating tunnel, and seldom related to embedded tunnel, in the less research available, Wlliams et al. [28] calculated the dynamic response of a long, submerged, semi-cylindrical shell structure using Green's function approach. Chen XiangHong [29] studied the complete solution of embedded tunnel using force method by considering the dynamic earth pressure and water pressure separately.

In this study, two factors of hydrodynamic pressure and the soil resistance were considered simultaneously. The first factor considered was calculated using conformal mapping method, and the second one was viewed as Winkler foundation. Consequently, the reasonable design concepts applicable to the design of circular tunnel structure in high permeable stratums and to the evaluation of the effects of water pressure and soil resistance required for maintaining the stability of the tunnel face were suggested.

2. Theoretical analysis of hydrodynamic pressure

2.1 Wave equations

Firstly, we ignore the interaction of soil and water, a circular cavity with radius r in a fully saturated, isotropic, homogeneous, and semi-infinite porous aquifer is shown in Figure 1. For a compressible inviscid fluid, the two-dimensional vibration-induced hydrodynamic pressure satisfies the wave equation.

$$\nabla^2 p - \bar{k}^2 \ddot{p} = 0 \tag{1}$$

Where, $\bar{k} = 1/c$ is the compressible wave number, c is the wave velocity in water; $\nabla^2 = \partial^2/\partial x^2 + \partial^2/\partial y^2$ is the Laplace operator; dot notation indicates partial differentiation with respect to time.

The boundary conditions of the analytical model are defined as

$$\partial p/\partial n = -\rho \ddot{U} \tag{2a}$$

$$p = 0 \tag{2b}$$

Where, n denotes the unit normal, correspond to the inward normal direction to cavity; ρ is the mass density of fluid; $\ddot{U}$ is normal components of acceleration of the cavity.

2.2 Conformal mapping

The water surface and the cavity circumference in z-plane can be mapped conformably onto two circles of radius 1 and a, in w-plane the mapping function may be expressed as:

$$\psi = u + vi = \frac{z + iA}{z - iA} \tag{3}$$

In which, $A = h \bullet \dfrac{1 - a^2}{1 + a^2}$, $u = \dfrac{x^2 + y^2 - A^2}{x^2 + (y - A)^2}$, $v = \dfrac{2Ax}{x^2 + (y - A)^2}$ is the real and imaginary part of complex variable ψ,

$a = \dfrac{h}{r} - \sqrt{\dfrac{h^2}{r^2} - 1}$ is the radius of cavity in the w-plane, h is the depth of cavity center below the water surface.

Given the boundary of cavity in w-plane is discretized with local coordinates ξ, η and the nodes at the boundary of cavity face are denoted with $\hat{u}$, $\hat{v}$. Introduce the mapping function $N(\xi, \eta)$ and the nodal pressure function $\hat{p}$, we get the nodal coordinate and pressure as follows

$$u(\xi,\eta) = N(\xi,\eta) \bullet \hat{u}$$
$$v(\xi,\eta) = N(\xi,\eta) \bullet \hat{v} \tag{4}$$

$$p(\xi,\eta) = N(\xi,\eta) \bullet \hat{p} \qquad (5)$$

The hydrodynamic pressure in w-plane also satisfy the Laplace equation, for simplifying the contents of the chapter, the transformation formulas of Equations (1), (2a) and (2b) will be omitted. By applying the Jacobian matrix $[J(\xi,\eta)]$ and the method of weighted residual, the solution of differential equation of hydrodynamic pressure is equivalent to the weak-form solution as the following integral equation

$$\int_{\Gamma} \nabla\phi\nabla p\,d\Gamma + \bar{k}^2 \int_{\Gamma} \phi\ddot{p}\,d\Gamma + \rho\int_{L} \phi\ddot{U}\,dL = 0 \qquad (6)$$

Where, ϕ is the weighting function which can be expressed as $N(\xi,\eta)$; Γ denotes the fluid domain, and L denotes the boundary of cavity.

2.3 Solution

Given an isoparametric element with four nodes (i,j,k,l), the hydrodynamic pressure is $\hat{p}_i, \hat{p}_j, \hat{p}_k, \hat{p}_l$. For an arbitrary point of the element, the hydrodynamic pressure can be expressed as

$$p(\xi,\eta) = \begin{bmatrix} N_i(\xi,\eta) & N_j(\xi,\eta) & N_k(\xi,\eta) & N_l(\xi,\eta) \end{bmatrix} \bullet \{\hat{p}_m\}^T_{m=i,j,k,l} \qquad (7)$$

Substituting Equation (7) in Equation (6), we get

$$\int_{\Gamma} \left\{ \left[\frac{\partial N_m}{\partial u}\frac{\partial N_n}{\partial u} + \frac{\partial N_m}{\partial v}\frac{\partial N_n}{\partial v} \right] \bullet \{\hat{p}_m\}^T + \bar{k}^2 [N_m]^T [N_m]\{\ddot{\hat{p}}_m\}^T \right\} d\Gamma + \rho\int_{L}[N_m]^T\{\ddot{U}\}dL \bigg|_{m,n=i,j,k,l} = 0 \qquad (8)$$
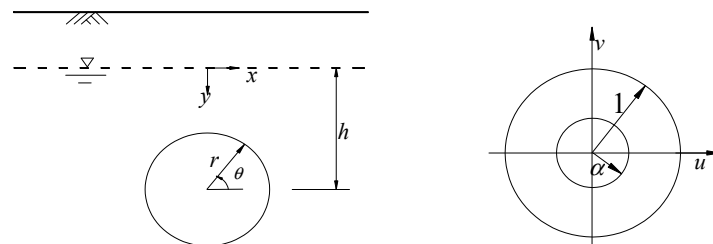

Figure.1 The circular cavity in a semi-infinite aquifer and the related conformal mapping in z-plane into two concentric circles in w-plane

2.4 Illustration of hydrodynamic pressure

According to the deduced Equation (8), the hydrodynamic pressure is related to the vibration acceleration $\ddot{U}$. Assuming a circular cavity deforms as a function of parabola along the direction of loadings, the mass density of water ρ =1000 kg/m³, acoustic speed in water c =1400 m/s.

In order to analyze the hydrodynamic pressure distribution properties with vibration frequency, the water body is discretized with four-node square elements as $\Delta\theta = 1^o$, and the hydrodynamic pressure over the cavity are studied and depicted for excitation frequency ranging from 0-1000 Hz. Supposing the hydrodynamic pressure is normalized with respect to the hydrostatic pressure ρgh, Figure 2 and Figure 3 show the maximum normalized hydrodynamic pressure for water depth of 6 m, 10 m, 20 m and the acceleration amplitude of 0.1, 0.3 and 0.4 respectively. As can be seen from Figure 2, some changes of the hydrodynamic pressure peaks and its location in the higher frequency range take place; the normalized hydrodynamic pressures are sensitive to the water depth, i.e., the hydrodynamic pressure decrease with the increase of water depth, the main vibration frequency delays meanwhile, moreover, the hydrodynamic pressure developed slowly in the low vibration frequency and the tendency became more obviously with the depth. From Figure 3, the maximum hydrodynamic pressure increases with the excitation acceleration amplitude.
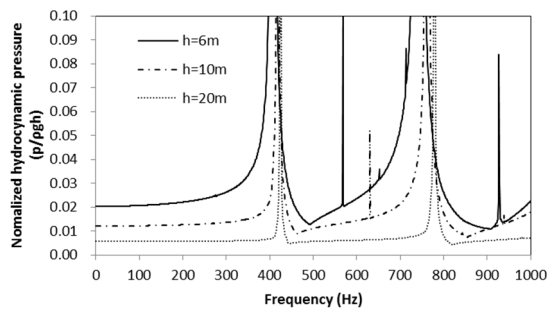
Figure.2 The maximum normalized hydrodynamic pressure .vs. the excitation frequency
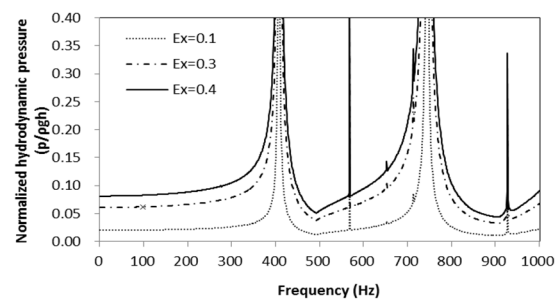

Figure.3 The maximum normalized hydrodynamic pressure .vs. the excitation frequency

Furthermore, if we take out three frequency points of 60Hz, 200Hz and 380Hz and draw it in Figure 4, from which we can found that: in the range of $1 < h/r < 2$, the absolute normalized hydrodynamic pressure $p/\rho g h$ over the cavity face increase with the dimensionless parameter h/r. While a decrease tendency happens in the range of $h/r > 2$.
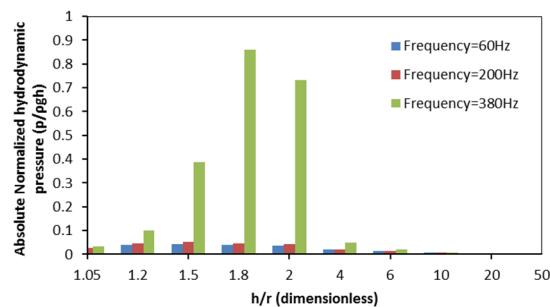

Figure.4 Absolute normalized hydrodynamic pressure on the tunnel face .vs. h/r ratio as the excitation vibration amplitude coefficient Ex=0.1

3. Dynamic response of embedded tube tunnel in high permeable stratum

3.1 Simplified model for tunnel

For simplifying the calculation of tunnel deformation and stress induced by the vibration loadings, based on Kirchhoff-love assumption and the method of water soil calculation separately, we take the tunnel structure as elastic foundation beam with less deformation, as shown in Figure 5. At a certain vibration frequency, the tunnel axis control equation can be expressed as.

$$EI\left[\frac{d^5 w(\theta)}{d\theta^5} + 2\frac{d^3 w(\theta)}{d\theta^3} + (1+\lambda)\frac{dw(\theta)}{d\theta}\right] = r_0^4 p'(\theta) \tag{9}$$

Where, $\lambda = k_e r_0^4 / EI$, EI is the equivalent Flexural rigidity, r_0 is the tunnel shaft radius, k_e is the equivalent elastic foundation coefficient, and the superscript number sign denotes the derivative with respect to angle θ.
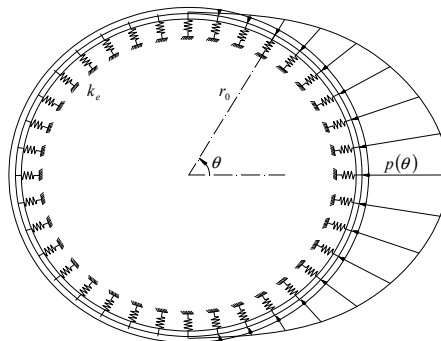
Figure 5 Simplified calculation model for tunnel

Referring to straight beam bending theory, the relative axial deformation v, rotation angle φ, bending moment M, shearing force Q and axial force N in Polar coordinate system is

$$v(\theta) = -\int w(\theta)d\theta + C_0 \tag{10a}$$

$$\varphi(\theta) = \frac{1}{r_0}\left[\frac{dw(\theta)}{d\theta} - v(\theta)\right] \tag{10b}$$

$$M(\theta) = \frac{EI}{r_0^2}\left[\frac{d^2w(\theta)}{d\theta^2} + w(\theta)\right] \tag{10c}$$

$$Q(\theta) = \frac{EI}{r_0^3}\left[\frac{d^3w(\theta)}{d\theta^3} + \frac{dw(\theta)}{d\theta}\right] \tag{10d}$$

$$N(\theta) = r_0 p(\theta) - \frac{EI}{r_0^3}\left[\frac{d^4w(\theta)}{d\theta^4} + \frac{dw^2(\theta)}{d\theta^2} + \lambda w(\theta)\right] \tag{10e}$$

In generally, the solution of the governing differential equation (9) is obtained

$$w(\theta) = B_1 + B_2 sh\alpha\theta\cos\beta\theta + B_3 ch\alpha\theta\cos\beta\theta + B_4 sh\alpha\theta\sin\beta\theta + B_5 ch\alpha\theta\sin\beta\theta + f(\theta) \tag{11}$$

In which, B_1 to B_5 and C_0 are the constant coefficients, that can be solved with the boundary conditions; $f(\theta)$ denotes the special solution; and the parameters of α and β is

$$\alpha = \sqrt{\frac{1}{2}\sqrt{1+\lambda} - \frac{1}{2}}, \quad \beta = \sqrt{\frac{1}{2}\sqrt{1+\lambda} + \frac{1}{2}}, \quad \lambda = \frac{k_e r_0^4}{EI}$$

By introducing the initial conditions of symmetric system, the equations (10) and (11) can be expressed as follows.

$$S_l = \mathrm{T} \bullet S_0 + S^* \tag{12}$$

In which, $S = \{w \quad v \quad \varphi \quad M \quad Q \quad N\}$, T is the field matrix for the circular arc beam.

3.2 Calculation parameters
As in Figure 5, a circular tunnel with 3 m radius and 0.3 m wall thickness is located in a high permeable stratum. The region is mainly dominant by saturated sandy gravel with high permeability. Table 1 shows us the main material properties of the tunnel lining.

Table 1 Material properties of tunnel lining

Properties	Values
Elastic modulus (Gpa)	30
Density (kg/m^3)	2 500
Poisson ratio	0.2

To simplify the calculation, we ignore the frictional resistance between soil and structure, the radial contact counterforce is only considered for the analysis of the elastic foundation beam, and the spring coefficient for representing the soil stress-strain response is 20Mpa/m.

Considering that the vibration frequency of tunnel structure in sandy gravel (Tao Lian-jin et al. [30,31]; Su Qi et al. [32]) caused by train operation distributes in the range from 0~120 Hz, generally ranges from 20~90 Hz by tunnel excavation, and is more less than 50 Hz under seismic vibration. So, without loss of generality, we choose the vibration frequency to be 5 Hz; the maximum vibration acceleration amplitude to be 0.3 and the boundary conditions is.

$$\begin{cases} w(0) = v(0) = M(0) = 0 \\ v(\pi/2) = \varphi(\pi/2) = Q(\pi/2) = 0 \end{cases} \tag{13}$$

Then the effects of hydrodynamic pressure on the response of embedded tube tunnel can be determined from equations (12) and (13) by MATLAB programming.

3.3 Calculation solutions

Based on the simplified circular beam model and calculation parameters, take one fourth of structure for example, the deformation and internal force of tunnel induced by hydrodynamic pressure are shown in Figure 6. As to the problem of water depth, Figure 7 and Figure 8 show us the dynamic response law of structure under different water depths ranging from 10 m to 50 m considering soil-tunnel interaction.
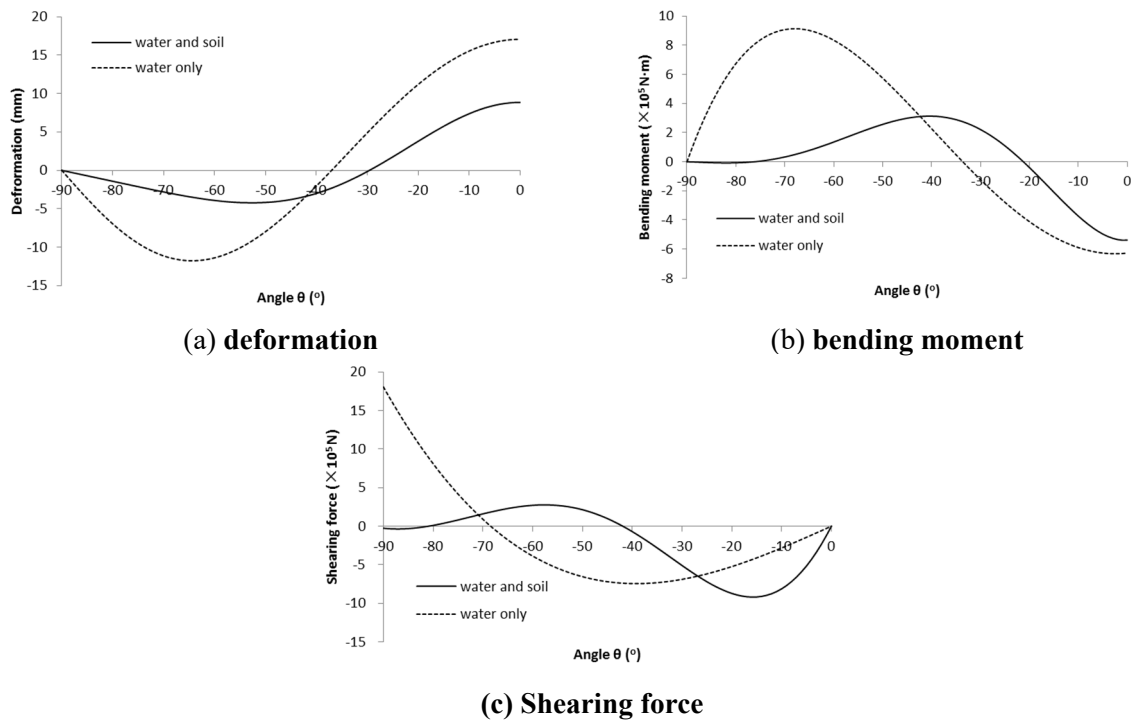

(a) **deformation**   (b) **bending moment**

(c) **Shearing force**

Figure.6 Comparation of dynamic response curves of structure for vibration frequency f=5 Hz, h=10 m

(a) **deformation**

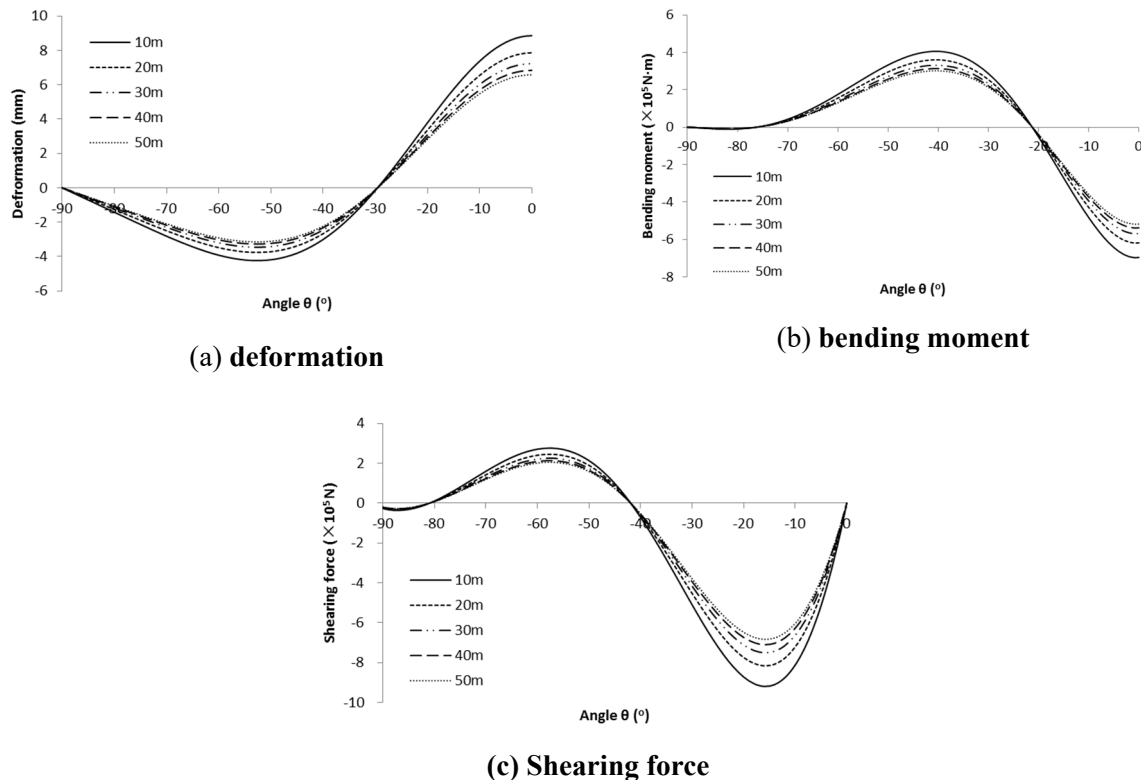

(b) **bending moment**

(c) **Shearing force**

Figure.7 Dynamic response curves of structure under different water depth
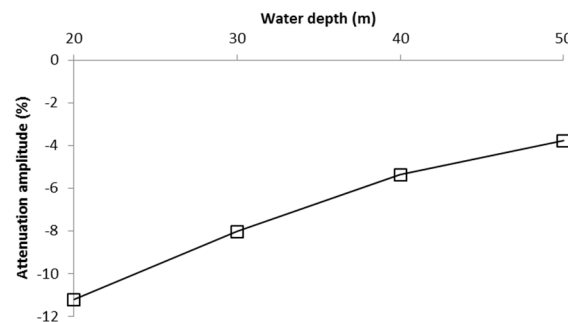

Figure.8 Percentage of deformation attenuation with water depth from 10 m to 50 m

From Figure 6 we can see: soil-structure interaction plays an important role in deducing the detrimental effects of hydrodynamic water pressure on tunnel; meanwhile, improving the external soil can decrease the deformation of structure and reduce the risk of water leakage, which is helpful for the operation of shield tunnel especially.

In Figure 7, values of structural dynamic response decrease with water depth, and the percentage of attenuation decrease gradually with the increase of water depth from Figure 8. So, the optimal design for embedded tube tunnel in high permeable stratum is needed considering the effects of water depth and soil resistance.

4. Conclusions

The dynamic tunnel structure in high permeable stratum is investigated. The equations of hydrodynamic pressure and tunnel–water–soil system were first generalized, results of hydrodynamic pressure relates not only to the acceleration of structure, but also to vibration frequency and water

depth; the impedances of soil play an important role for reducing the detrimental effects of hydrodynamic pressure. The main conclusions remain valid for the special conditions of soil and water calculated separately in the simplified model: (1) the calculated hydrodynamic pressure relates to the vibration frequency by conformal mapping method and varies with the water depth and structural acceleration. (2) The dimensionless hydrodynamic pressure $p/\rho gh$ increases firstly and then decreases with the dimensionless parameter h/r. (3) As for the vibrations with low frequency, effects of water resonance will not be considered in the dynamic analysis of underwater system. (4) The property of ground motion affects drastically the operation conditions of tunnel, especially for the shied tunnel. (5) The dynamic response reduces nonlinearly with the water depth and the attenuation percentage decrease nonlinearly in the meanwhile.

References

[1]   K.H Park, J.G Lee, A Owatsiriwong. Seepage force in a drained circular tunnel: An analytical approach[J]. Canadian Geotechnical Journal, 2008, 45(03): 432-436.

[2]   K.H Park, A Owatsiriwong, J.G Lee. Analytical solution for steady-state groundwater inflow into a drained circular tunnel in a semi-infinite aquifer: a revisit[J]. Tunnelling and Underground Space Technology, 2007, 23(2): 206-209.

[3]   D Kolymbas, P Wagner. Groundwater ingress to tunnels - the exact analytical solution[J]. Tunnelling and Underground Space Technology, 2007, 22(1): 23-27.

[4]   Huang Fu-ming. A study on surrounding rockmass stability and stress characteristics of lining structure for undersea tunnels constructed by excavation method[D]. Being Jiaotong University, 2005.(in Chinese)

[5]   Harr, M.E. Groundwater and seepage[M]. McGraw-Hill, New York, 1962.

[6]   G Fernandez, T.A Alvarez. Seepage-induced effective stresses and water pressures around pressure tunnels[J]. Journal of Geotechnical Engineering, 1994, 120(1): 108-127.

[7]   E.I Tani, M. Circular tunnel in a semi-infinite aquifer[J]. Tunnelling and Underground Space Technology, 2003, 18(1): 49-55

[8]   In-Mo Lee, Seok-Woo Nam. Effect of tunnel advance rate on seepage forces acting on the underwater tunnel face[J]. Tunnelling and Underground Space Technology, 2004, 19(3): 273-281.

[9]   In-Mo Lee, Seok-Woo Nam. The study of seepage forces acting on the tunnel lining and tunnel face in shallow tunnels[J]. Tunnelling and Underground Space Technology, 2001, 16(1): 31-40.

[10] Seok-Woo Nam, Antonio Bobet. Liner stresses in deep tunnels below the water table[J]. Tunnelling and Underground Space Technology, 2006, 21(6): 626-635.

[11] Seok-Woo Nam, A. Bobet. Radial Deformations Induced by Groundwater Flow on Deep Circular Tunnels[J]. Rock Mechanics and Rock Engineering, 2007, 40(1): 23-39.

[12] T.C Carranza, J Zhao. Analytical and numerical study of the effect of water pressure on the mechanical response of cylindrical lined tunnels in elastic and elasto-plastic porous media[J]. International Journal of Rock Mechanics and Mining Sciences, 2009, 46(3): 531-547.

[13] Zhi-qiang Zhang, Bao-shu Guan, Wen-ge Qiu, et al. Research on Supporting Structure System of Yuanliangshan Railway Tunnel under High Water Head[J]. Chinese Journal of Rock Mechanics and Engineering, 2004, 23(5): 763-769.

[14] Xin-qiang Gao, Wen-ge Qiu, Yang Gao. 3D Numerical Simulation of the Lining Structure under High Water Pressure in Mountain Tunnel[J]. China Railway Science, 2005, 26(2): 29-33.

[15] A Bobet. Effect of pore water pressure on tunnel support during static and seismic loading[J]. Tunneling and Underground Space Technology, 2003, 18: 377-393.

[16] A Bobet. Lined Circular Tunnels in Elastic Transversely Anisotropic Rock at Depth[J]. Rock Mechanics and Rock Engineering, 2011, 44(2): 149-167.

[17]   Kang-he Xie, Gan-bin Liu, Zu-yuan Shi. Dynamic response of partially circular tunnel in viscoelastic saturated soil[J]. Soil Dynamic and Earthquake Engineering, 2004, 24(12): 1003-1011.

[18]   B Gatmiri, H Eslami. Scattering of Harmonic Waves by a Circular Cavity in a Porous Medium: Complex Functions Theory Approach[J]. International journal of geomechanics, 2007, 7(5): 371-381.

[19]   M.H Seyyed, S Kazemirad. Dynamic response of an eccentrically lined circular tunnel in poroelastic soil under seismic excitation[J]. Soil Dynamics and Earthquake Engineering, 2008, 28(4): 277-292.

[20]   Yi-Qun Tang, Zhen-Dong Cui, Xi Zhang, et al. Dynamic response and pore pressure model of the saturated soft clay around the tunnel under vibration loading of Shanghai subway[J]. Engineering Geology, 2008, 98(3): 126-132.

[21]   Y.M.A Hashash, J.J Hook, B Schmidt, et al. Seismic design and analysis of underground structures[J]. Tunnelling and Underground Space Technology, 2001, 16(4):247-293.

[22]   P.R Taylor, H.H Ibrahim, D Yang. Seismic retrofit of George Massey tunnel[J]. Earthquake Engineering and Structural Dy-namics, 2005, 34(4/5):519-542.

[23]   I Anastasopoulos, N Gerolymos, V Drosos, et al. Nonlinear response of deep immersed tunnel to strong seismic shaking[J]. Journal of Geotechnical and Geo-environmental Engineering，2007，13(39):1067-1090.

[24]   A Amorosi, D Boldini. Numerical modelling of the transverse dynamic behaviour of circular tunnels in clayey soils[J]. Soil Dynamics and Earthquake Engineering, 2009, 29 (6):1059-1072.

[25]   Kwak M K, Kim K C. Axisymmetric vibration of circular plates in contact with fluid[J].Journal of Sound and Vibration, 1991, 146(3):381-389.

[26]   Kwak M K. Hydroelastic vibration of circular plates[J]. Journal of Sound and Vibration, 1997, 201(3):293-303.

[27]   Zhou Ding, Cheung Y K. Vibration of vertical rectangular plate in contact with water on one side[J]. Earthquake engineering and structural dynamics, 2000, 29:293-710.

[28]   Wlliams A N, Mau S T. Earthquake Response of Submerged Circular Arch[J]. Journal of Waterway, Port, Coastal, and Ocean Engineering, 1988, 114(4):405-422.

[29]   Chen XiangHong. Study on the seismic response of large-scale submerged tunnel and auxiliary shaft [D]. Being Jiaotong University, 2013.

[30]   Tao Lianjin, Guo Fei, Huang Jun, et al. Field tests for environment vibration induced by shield tunneling in sand gravel layer[J]. Journal of Vibration And Shock, 2015,34(16):213-218.

[31]   Tao Lianjin, Guo Fei, Huang Jun, et al. Field tests for environment vibration induced by shield tunneling in sand gravel layer[J]. Journal of Vibration And Shock, 2015,34(16):213-218.

[32]   Su Qi, Su Bin, Tao Lianjin. The influence of shield construction and train operation on environment vibration in Sandy Cobble Stratum[M]. Beijing: tsinghua university press, 2015.